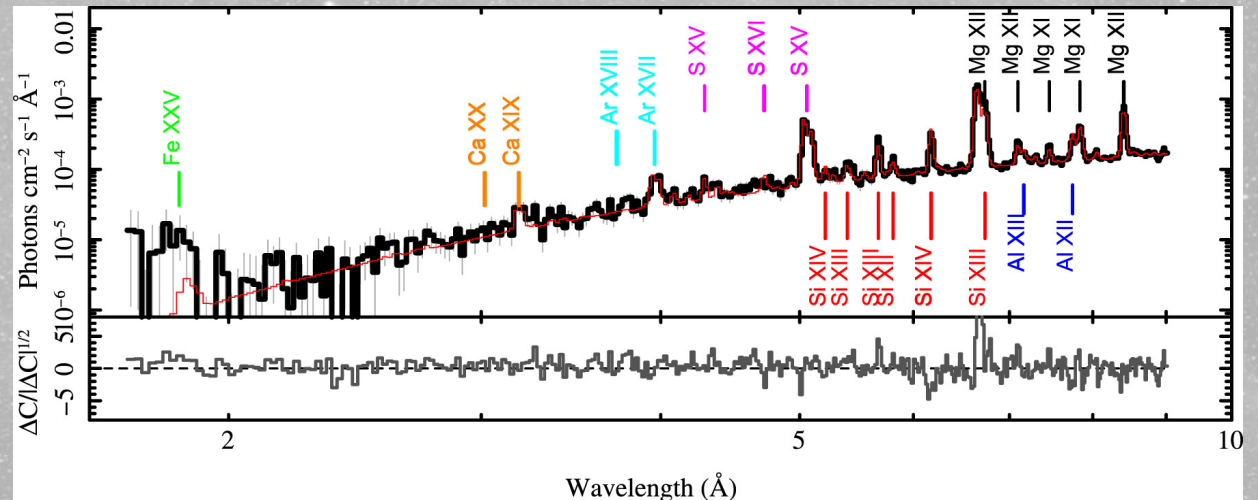
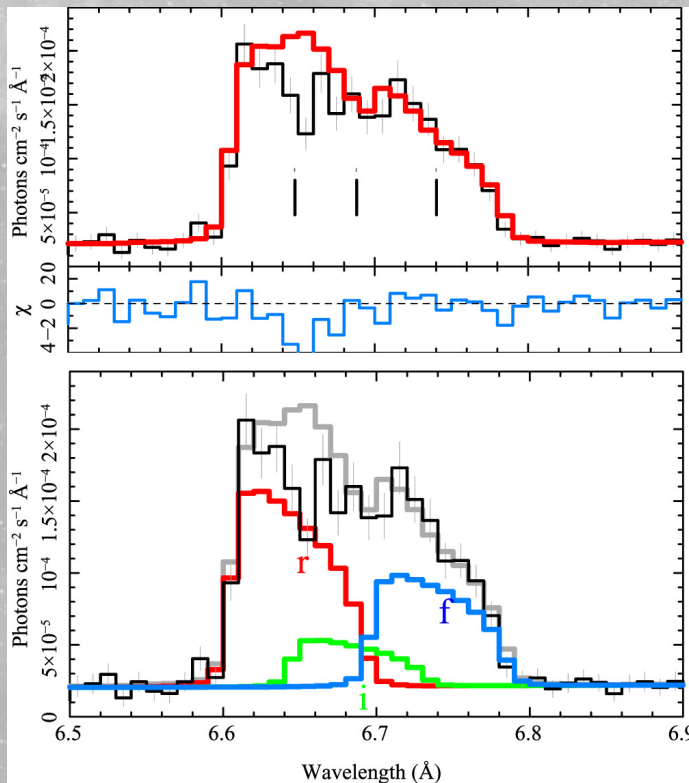




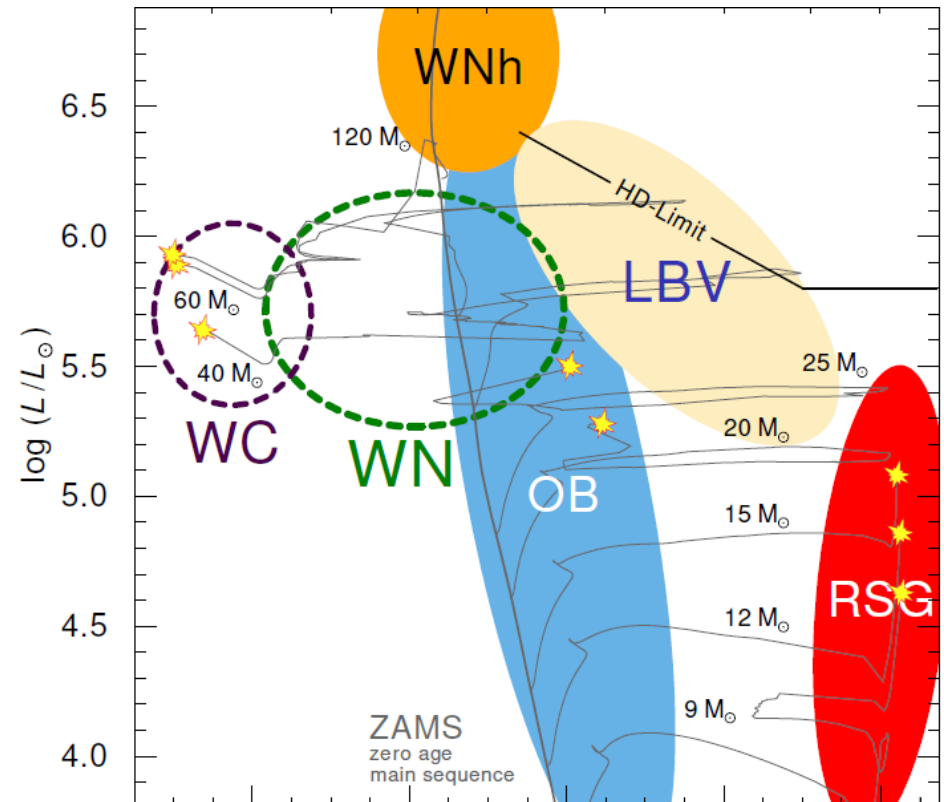
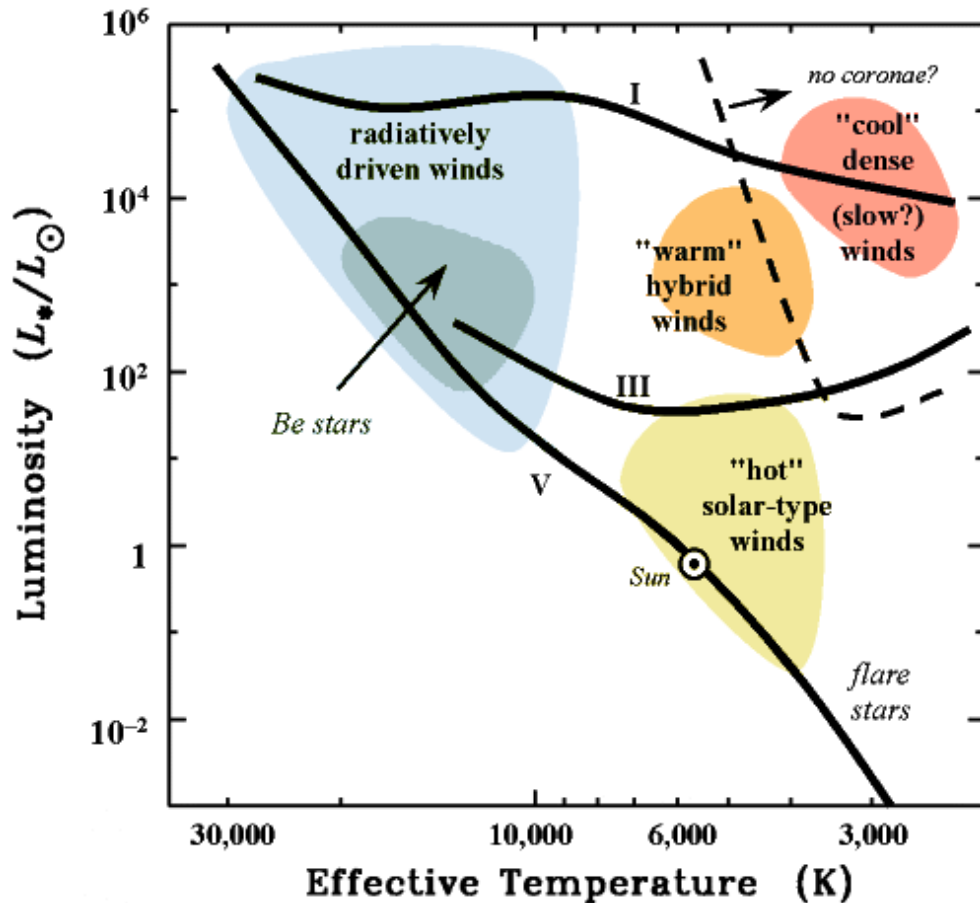
Modeling the X-ray Line Profile Shapes from Massive Star Winds

RICHARD IGNACE

*Department of Physics and Astronomy
East Tennessee State University*



Stellar Winds

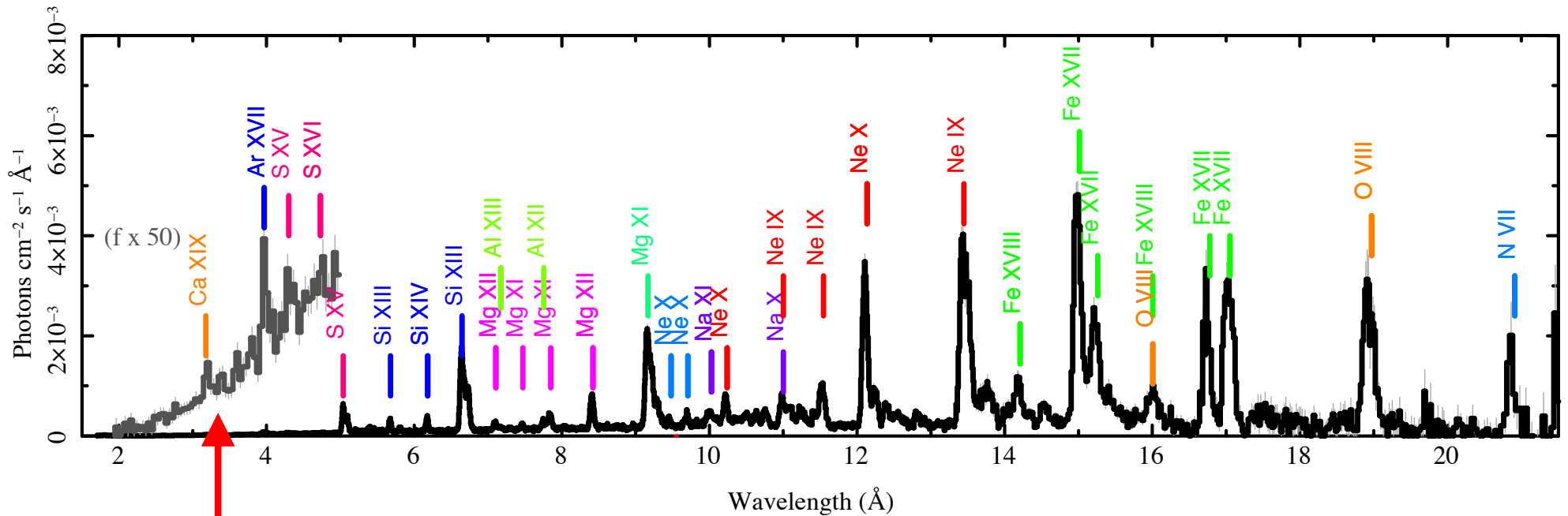


Massive star winds generally have broad lines of 1000s km/s

X-ray Production in Massive Stars

- **Colliding winds:** *[NOT DISCUSSED HERE]*
 - collision of winds from binary stars
 - or wind impact on companion star
- **Embedded wind shocks**
 - wind driving instabilities (stochastic structure)
- **Co-rotating Interaction Regions** *[NOT DISCUSSED HERE]*
 - no self-consistent modeling of this yet (organized structure)
- **Magnetospheres:**
 - magnetic confinement channels wind streams into head-on collisions ("self"-wind collision)
 - non-thermal emissions

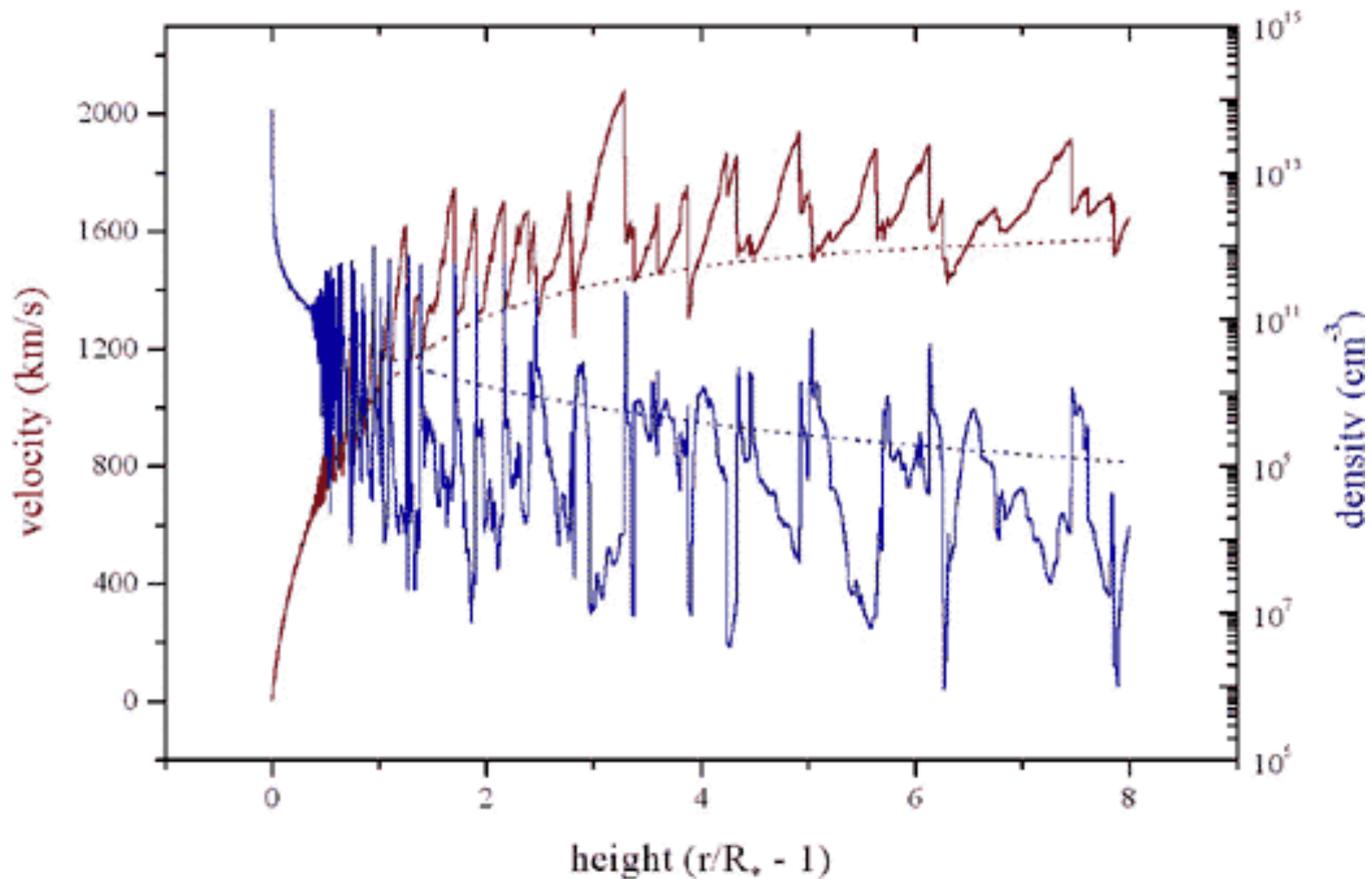
Chandra Large Program for Zeta Pup



- Fig from **Nichols+ 2021** (about 800ks) – rich emission line spectrum
- Detection of continuum emission at short wavelengths in with few lines (**Huenemoerder+ 2020**)
- Displays overall global spectral changes over ~20 years (**Cohen+ 2020** and this meeting)

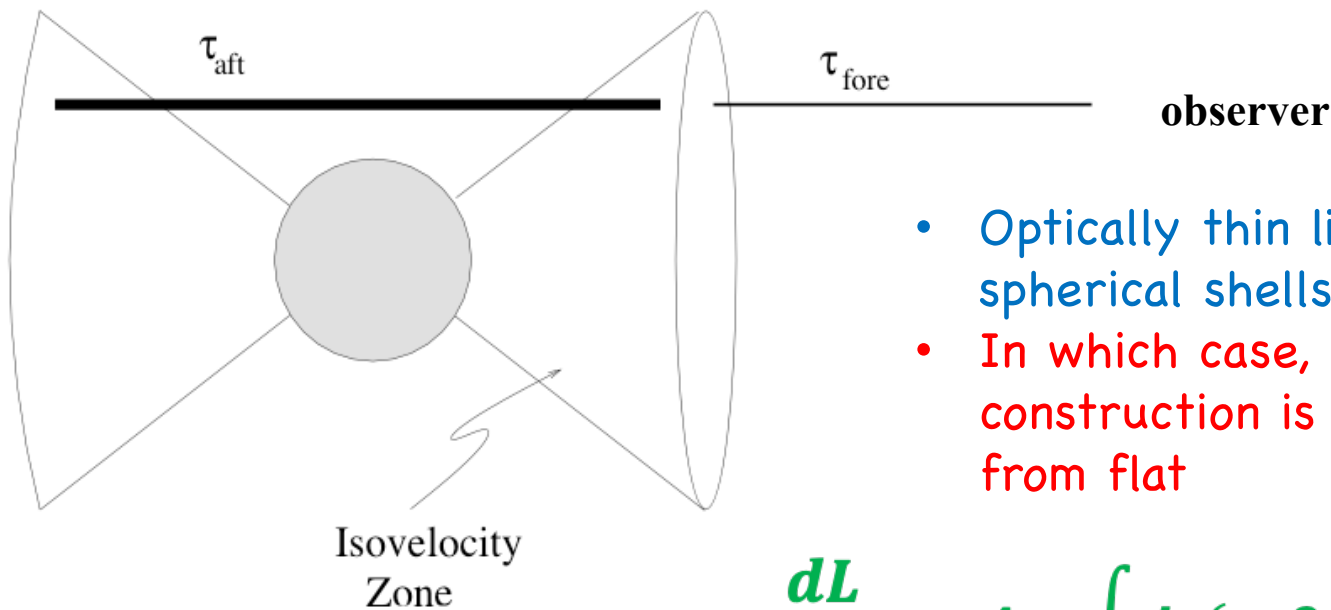
Underlying physical paradigm: Snapshot of the time-dependent structure for typical spherically symmetric O star wind

expectation of distributed hot gas



Line Profile Modeling: Optically thin Lines + Wind Photoabsorption

Geometry for a Constant Expansion Wind

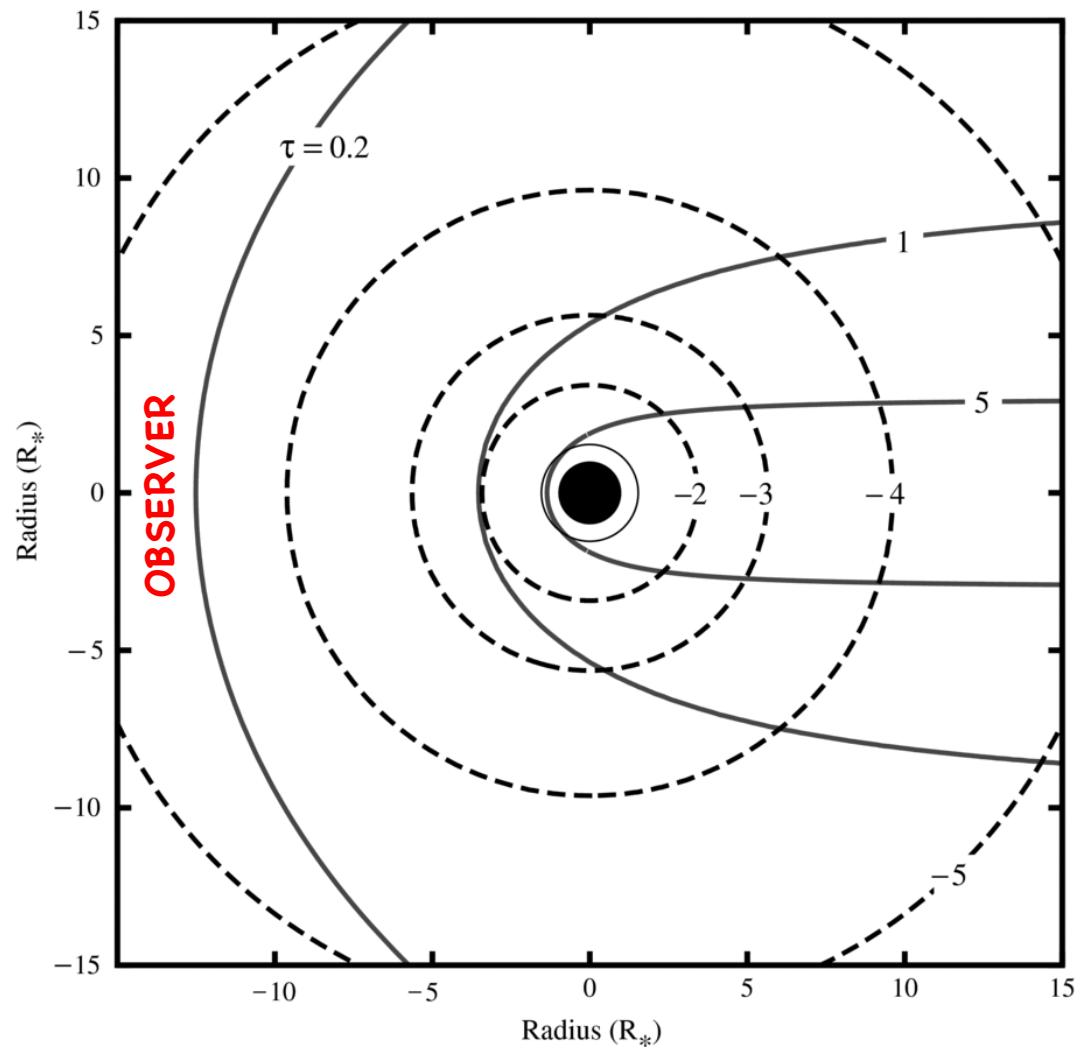
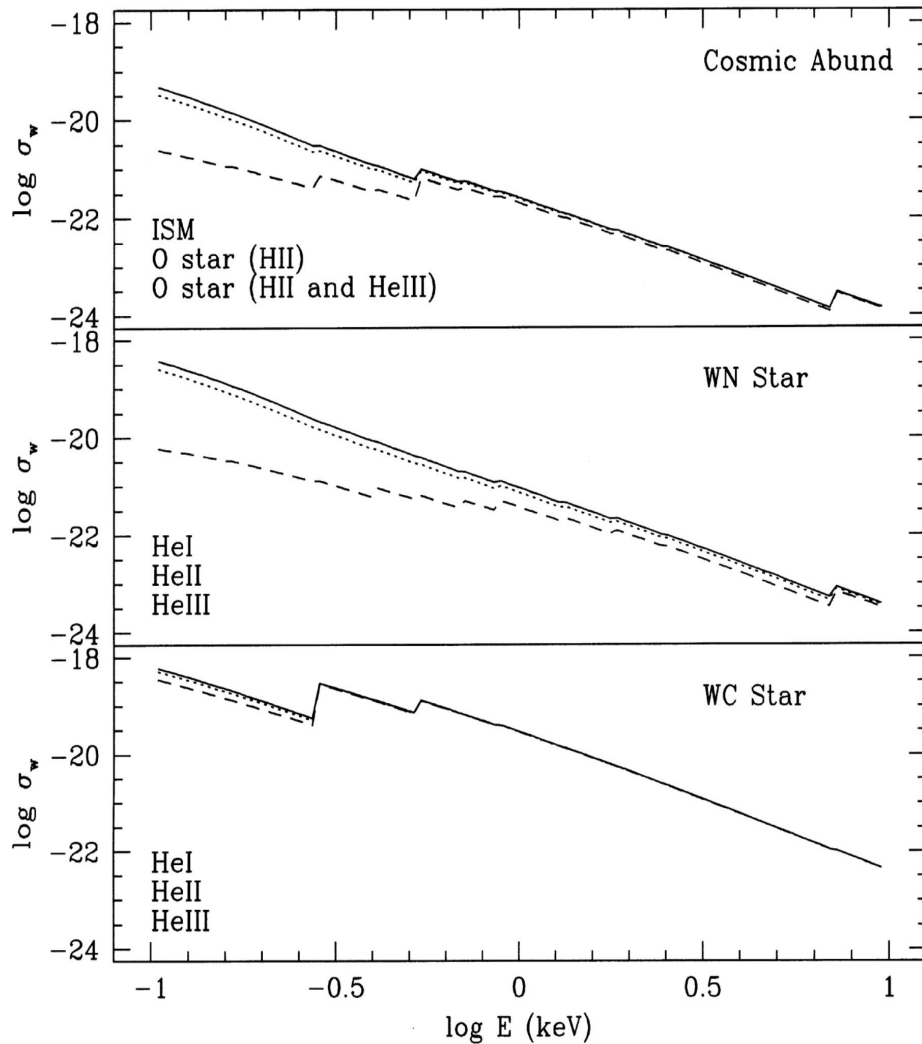


- Optically thin lines from spherical shells make flat-tops
- In which case, all profile construction is about deviation from flat

$$\frac{dL}{dv_{obs}} = 4\pi \int j_\nu(r, \theta, \phi) e^{-\tau} \frac{dVol}{v(r, \theta, \phi)}$$

resolved x-ray emission lines shapes can be blueward skewed

Photoabsorption

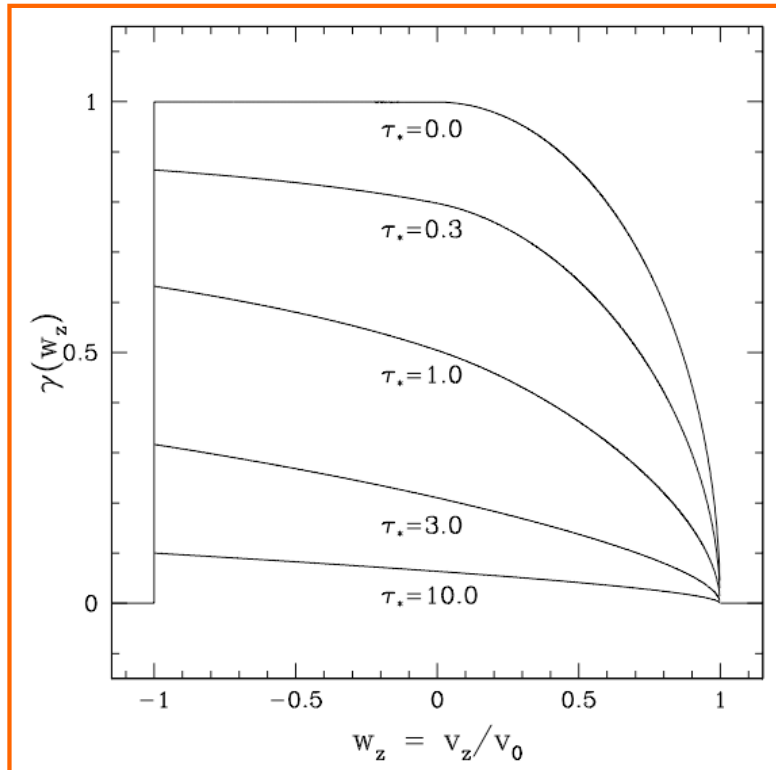


photoabsorption a function of density and of energy

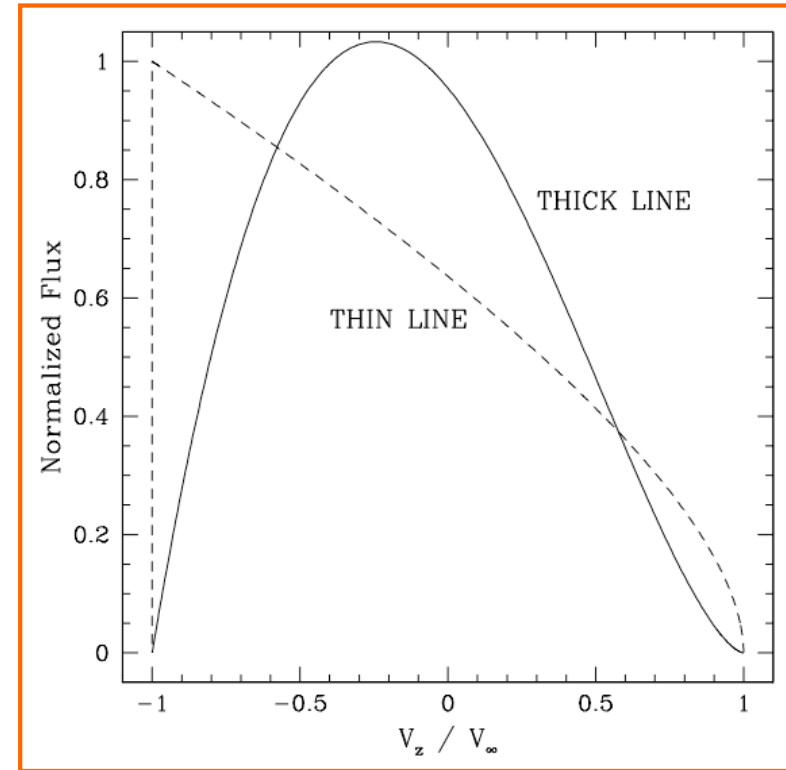
from Ignace+ 1999

from Leutenegger+ 2010

Examples of Simple Profiles



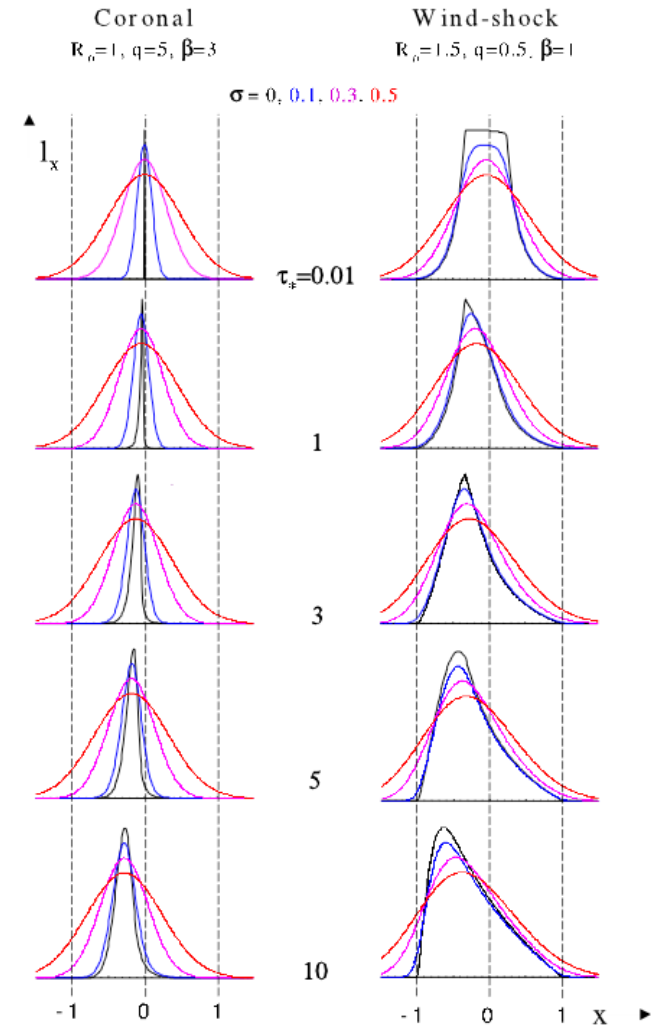
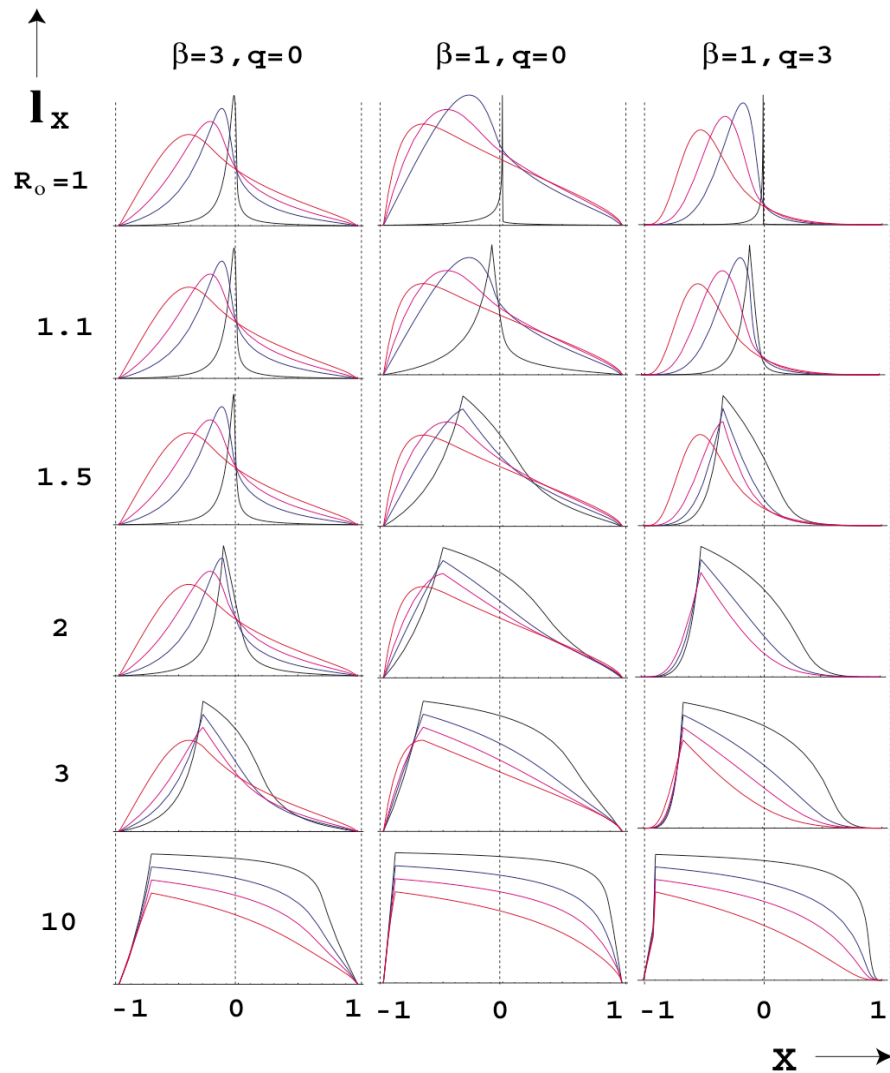
Optically thin lines with spherical constant expansion



Optically thick lines also with constant expansion

from Ignace 2001 and Ignace & Gayley 2003

Variation of Parameters (thin lines)

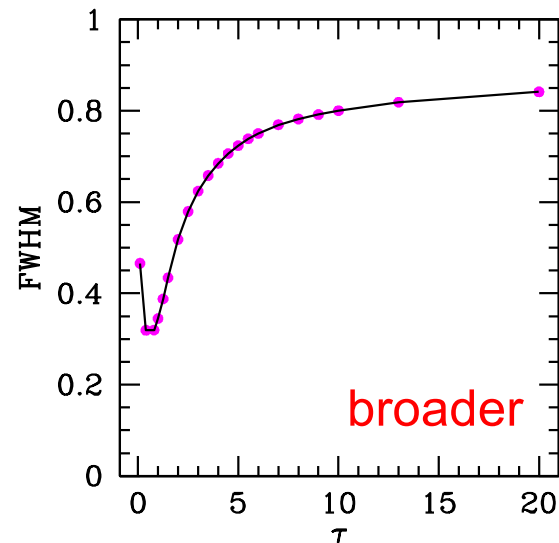
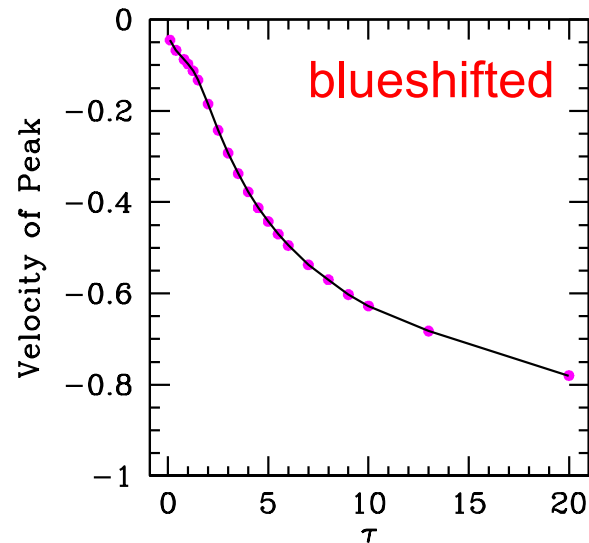


from Owocki & Cohen 2001

(beta is velocity law; R_0 is inner radius; q is a filling factor power-law exponent)

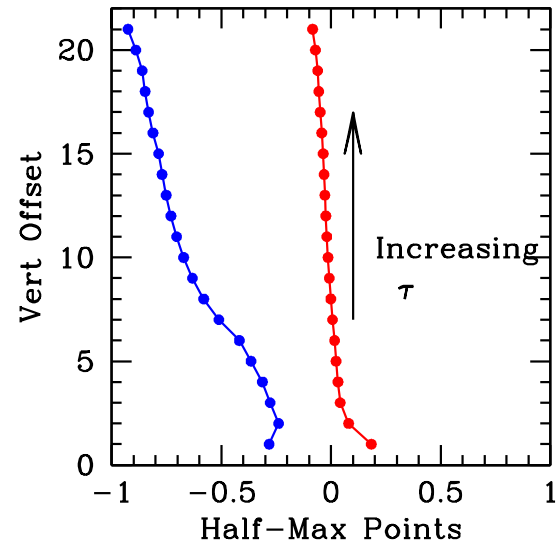
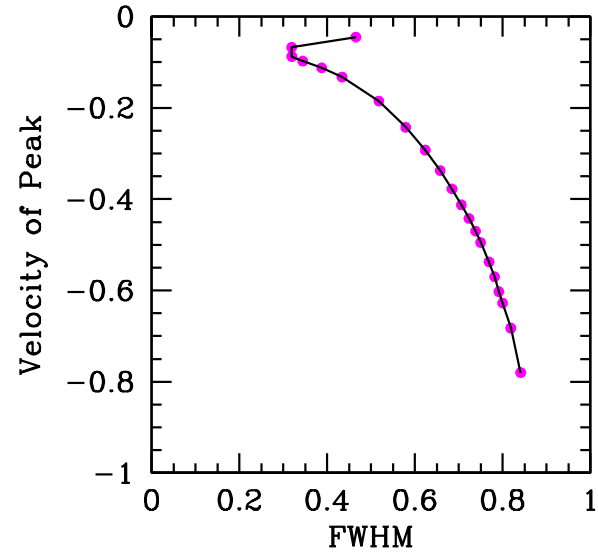
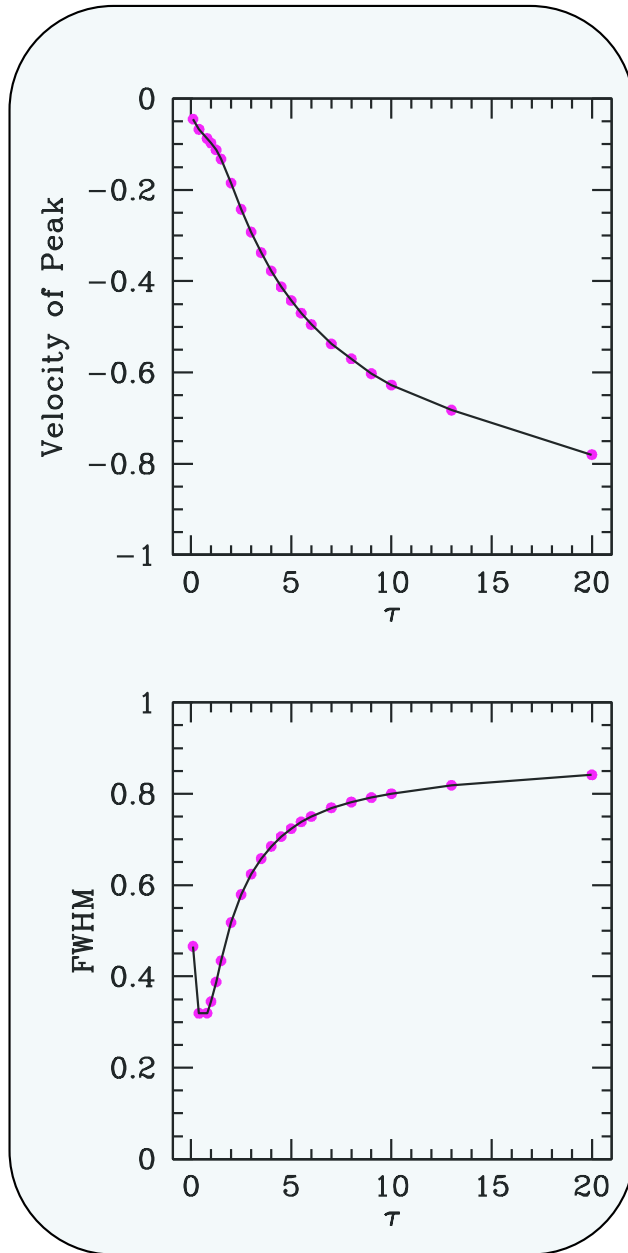
Trends in Line Profile Moments

- Smooth wind model
- Particular choice of wind velocity law
- Parametrized in terms of photo-absorptive optical depth, which is wavelength-dependent



THEORIST
PLOTS

Line Profile Moments: *OBSERVER PLOTS*

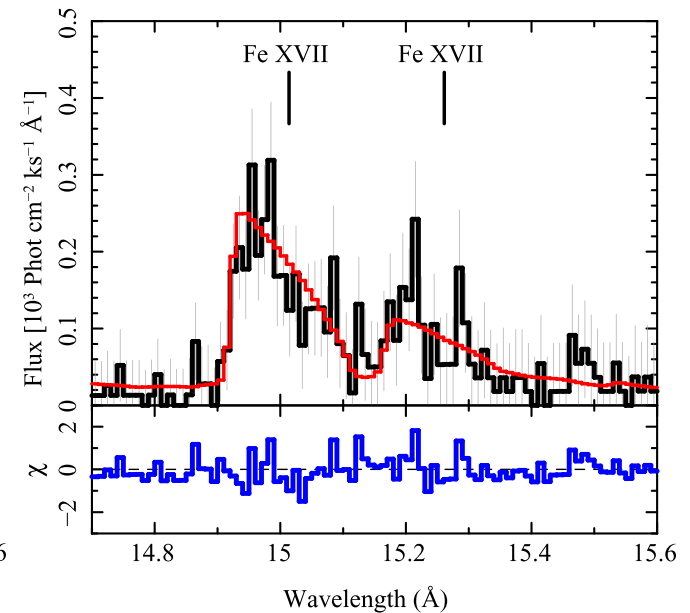
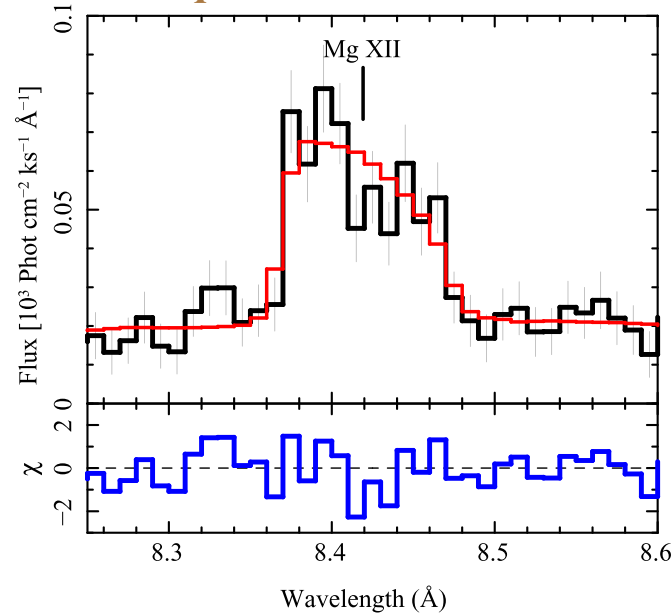
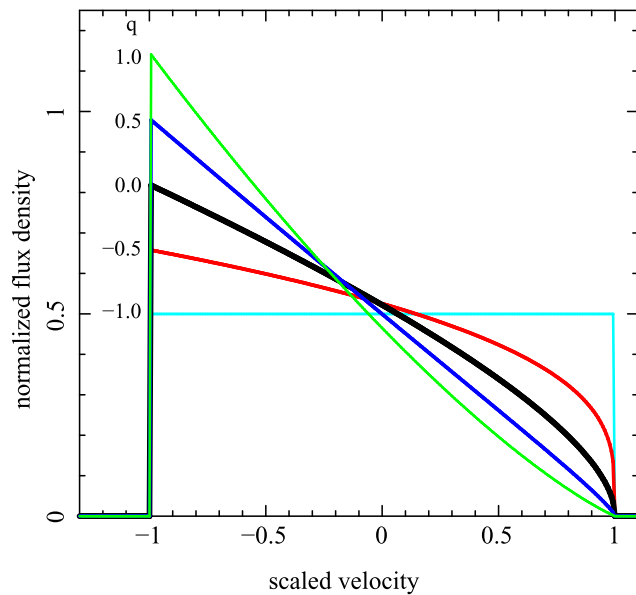


**Let's bounce through some
heuristic cases**

PROBING WOLF-RAYET WINDS: *CHANDRA*/HETG X-RAY SPECTRA OF WR 6

DAVID P. HUENEMOERDER¹, K. G. GAYLEY², W.-R. HAMANN³, R. IGNACE⁴, J. S. NICHOLS⁵, L. OSKINOVA³, A. M. T. POLLOCK^{6,7},
N. S. SCHULZ¹, AND T. SHENAR³

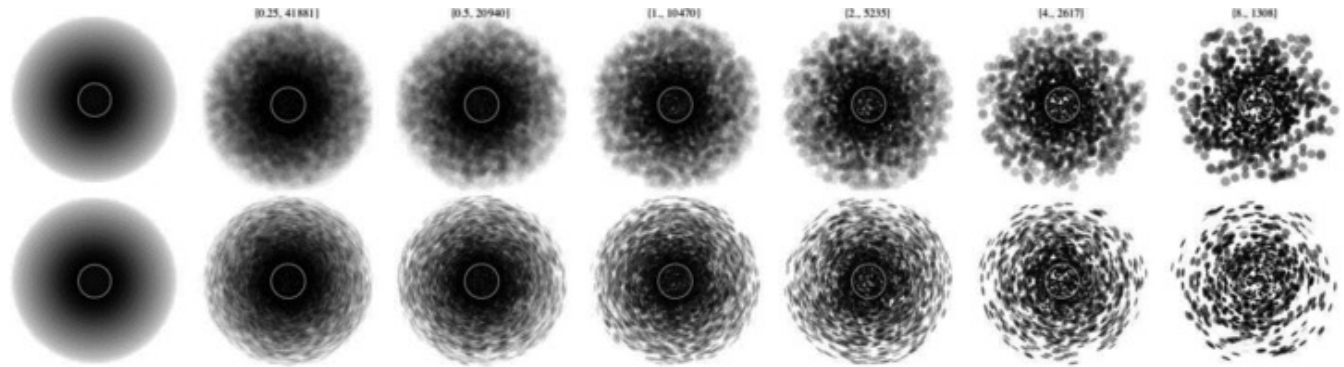
APPLICATION of model profiles for constant expansion



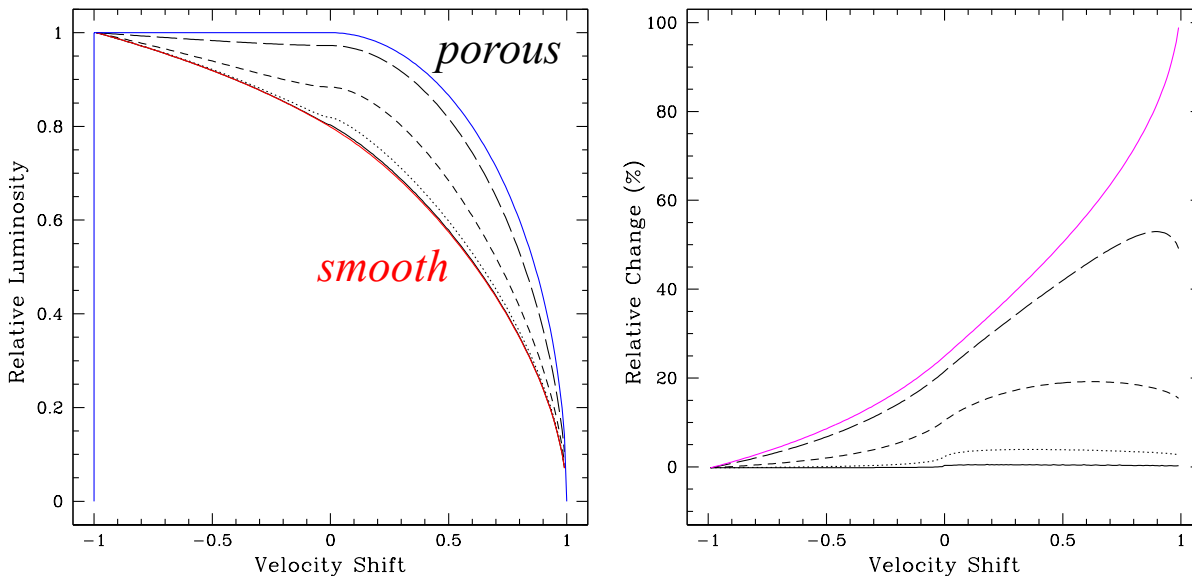
(line shape flux function)
$$f(w_z) = f_0 \left[\frac{\sqrt{1 - w_z^2}}{\arccos(-w_z)} \right]^{1+q}$$
 (q relates to radial filling factor distribution)

The value-added from profile modeling effort:
X-rays consistent with emerging from terminal speed flow

Porosity Effects



from Sundqvist 2012



from Ignace 2016

Figure 7: *Left:* An illustration of porosity effects on line profile shapes. The profiles are normalized to a peak value of unity. Red is for a smooth wind with $\tau_0 = 1$; blue is $\tau_0 = 0$. In black from solid to long dash are profiles with $h_\infty = 0.01, 0.1, 1.0$, and 10 , respectively, all with $\tau_0 = 1$. *Right:* Shown is the percent difference between normalized line profiles appearing in the left panel, with the red curve as the reference profile. Magenta (top) is the percent difference between the blue curve and the red one. The black curves are for winds with porosity corresponding to the lines in the left panel. Moving from small to large porosity lengths leads to a wind that is increasingly optically thin to photoabsorption for fixed τ_0 .

left to right: mean free path
between clumps
upper to lower: spherical
versus flat clumps

**upshot of porosity is to
“waste” absorption thru
spatial concentration that
allows avenues of escape**

Distribution Effects

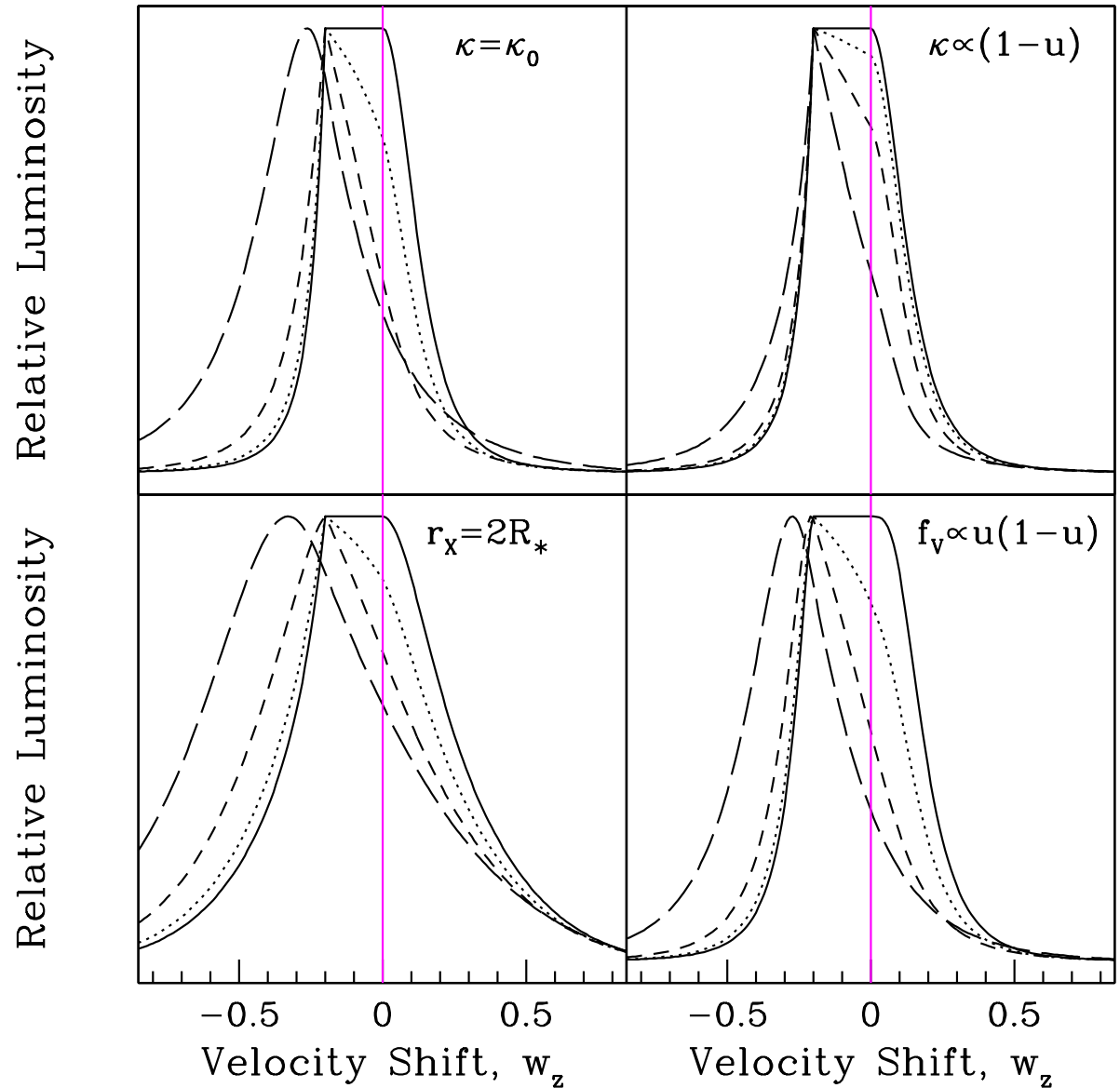
Choices!

Illustration of impacts from “recipe ingredients”

- All are peak normalized
- All lines assume $v \sim r$
- 4 curves for 4 absorbing optical depths
- upper for different absorbing distributions
- lower for different source distributions

Subtle differences

from Ignace 2016

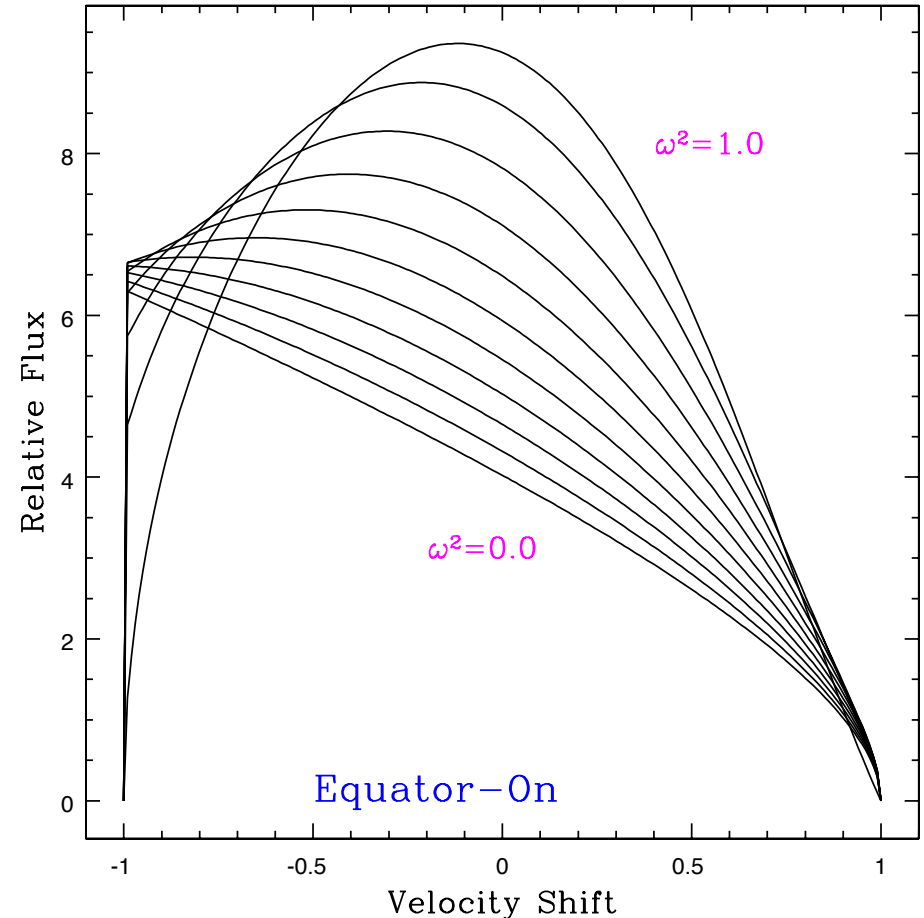
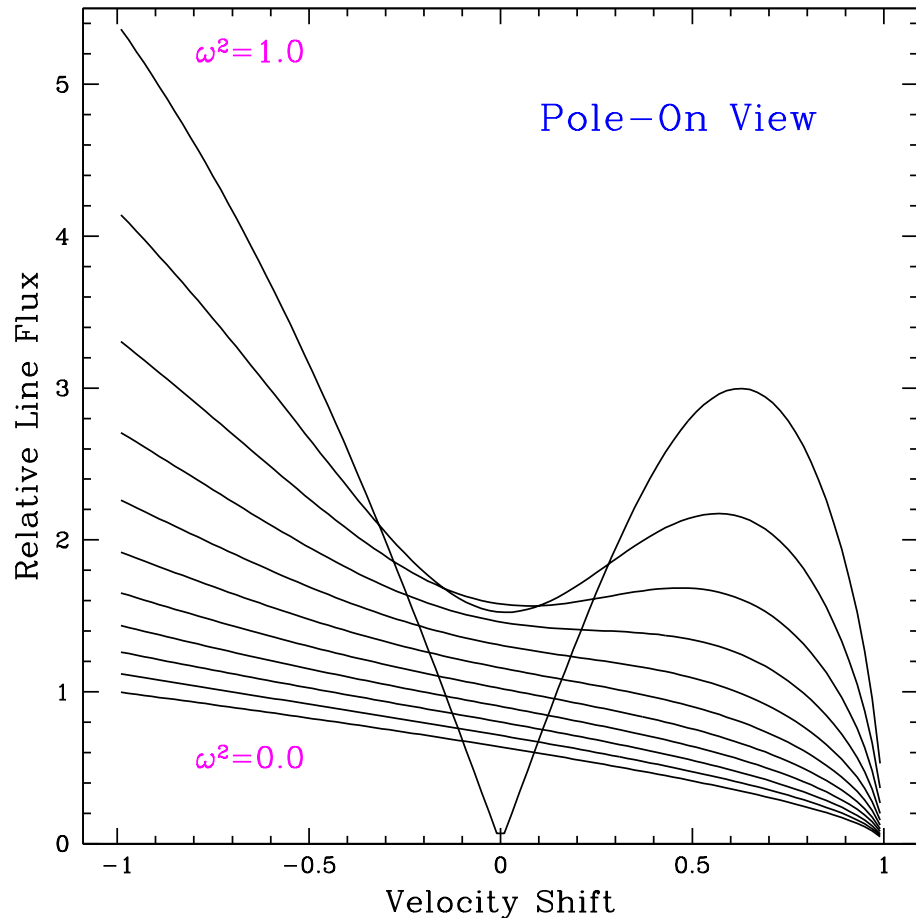


$$u = R_*/r$$

Figure 8: Example emission line profile shapes using $v(r) \propto r$, with each profile normalized to peak emission. Each panel shows four model profiles for $\tau_0 = 0$ (solid), 1 (dotted), 4 (short dash) and 14 (long dash). Upper left is for a constant photoabsorbing opacity; upper right is for one that varies with radius (see text). Lower panels are for constant absorption coefficient. Lower left is for $r_x = 1.4R_*$, and lower right is for a radius-dependent filling factor (see text).

Rotational Effects: *Wind Distortion*

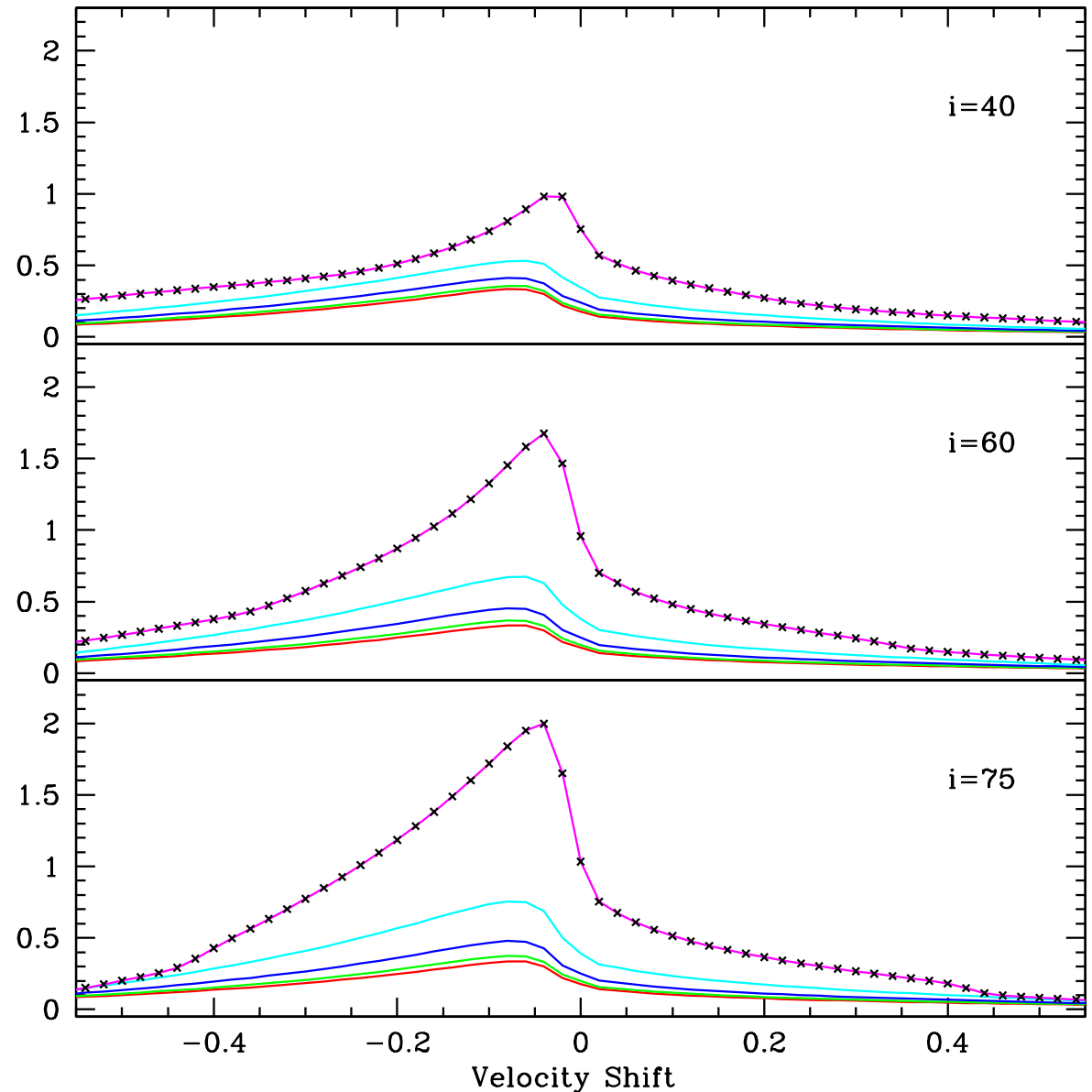
again: think “deviation from flat-top”



Using Owocki, Cranmer, & Gayley for distorted wind density and Maeder & Meynet global mass-loss dependence on rotation; constant expansion case

Rotational Effects: *V_{law}+Wind* *Absorption*

- no rotational velocity;
purely radial flow
- only rotationally distorted
density distribution
- and rotationally modified
terminal speed
- most prominent influence
is directional escape of
x-ray photons



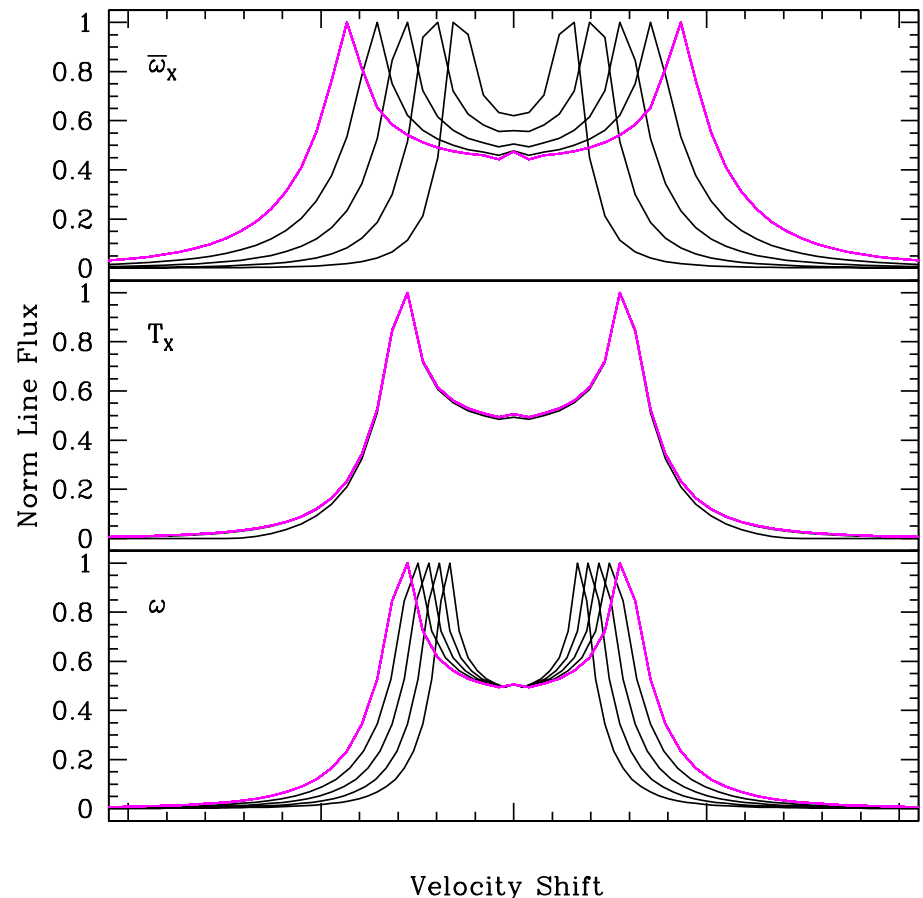
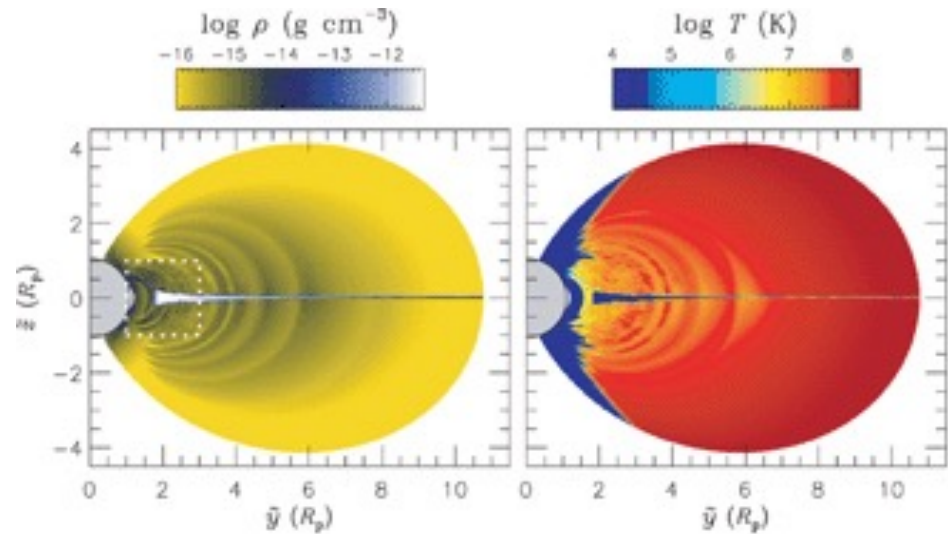
Now using a beta=1 velocity law

Rotational Effects:

Corotating Magnetosphere

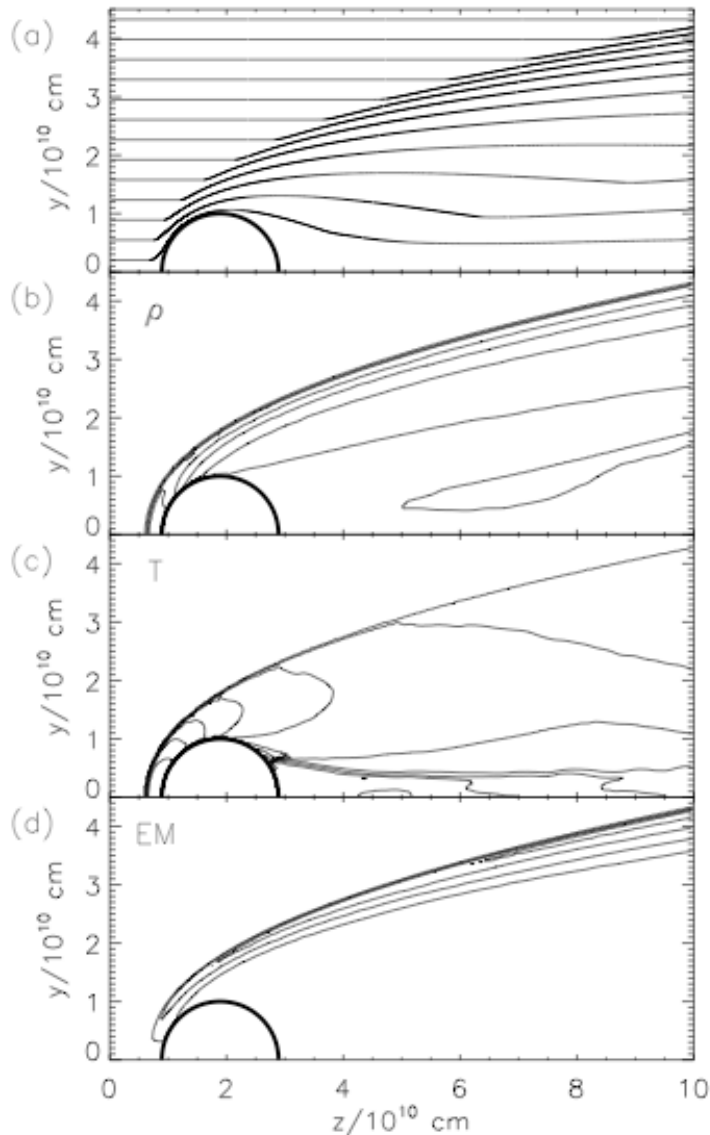
- Uses Rigid Field Hydrodynamics (RFHD) model of Townsend+ 2007
- semi-qualitative approach for an aligned dipole
- note isovelocity zones are planes seen edge-on, with left-right symmetry
- no radial flow or photoabsorption; pure solid-body velocity field

NOTE: thin line with spherical shell in solid body rotation is also flat-top



3D Effect: *Clump Bowshocks*

Cassinelli+ 2008



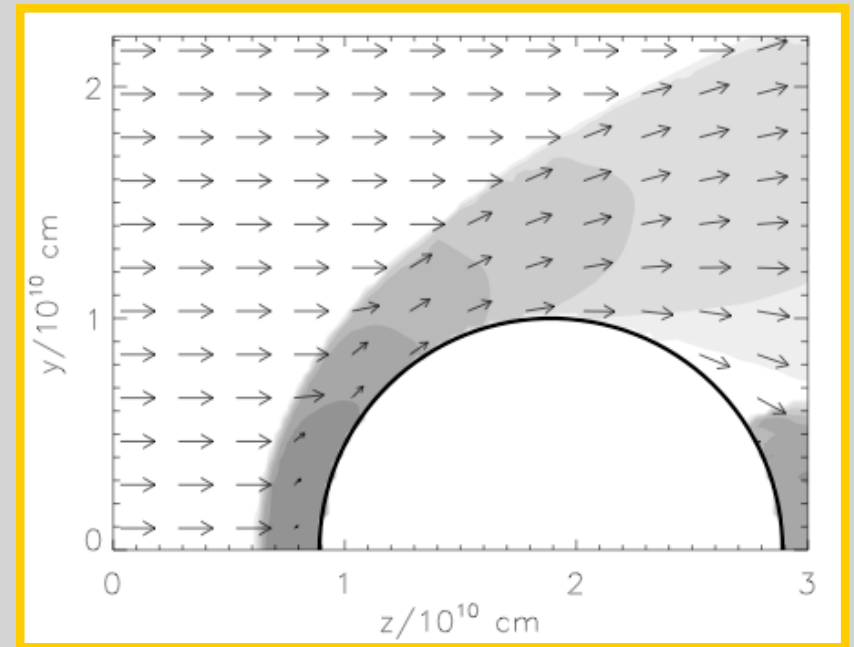
*Streamline
Flow*

Density

Temperature

*Emission
Measure*

Vector Flow



hydro assumes adiabatic cooling

X-RAY EMISSION LINE PROFILES FROM WIND CLUMP BOW SHOCKS IN MASSIVE STARS

R. IGNACE¹, W. L. WALDRON², J. P. CASSINELLI³, AND A. E. BURKE⁴

bowshock qualitatively a 1-sided bipolar outflow; which trends a double-horn profile

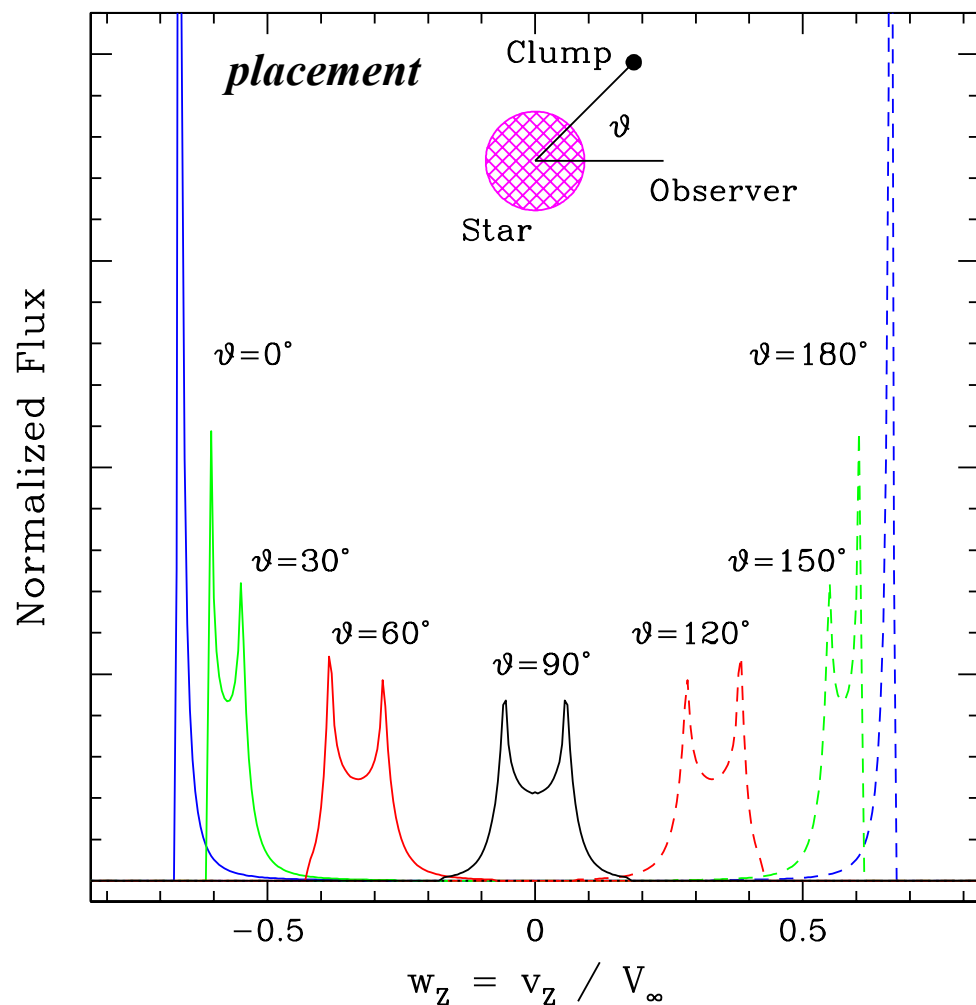


Figure 2. Inset (top center) shows the location of a clump at angle ϑ around the star from the observer's axis. The plot shows example emission line profiles, all normalized to have unit area, for individual clumps located at the indicated orientations. In each case the clump is at the same radius, and so all profiles have the same apex temperature T_A . Solid curves are for clumps on the near side of the star; dashed are for ones on the far side.

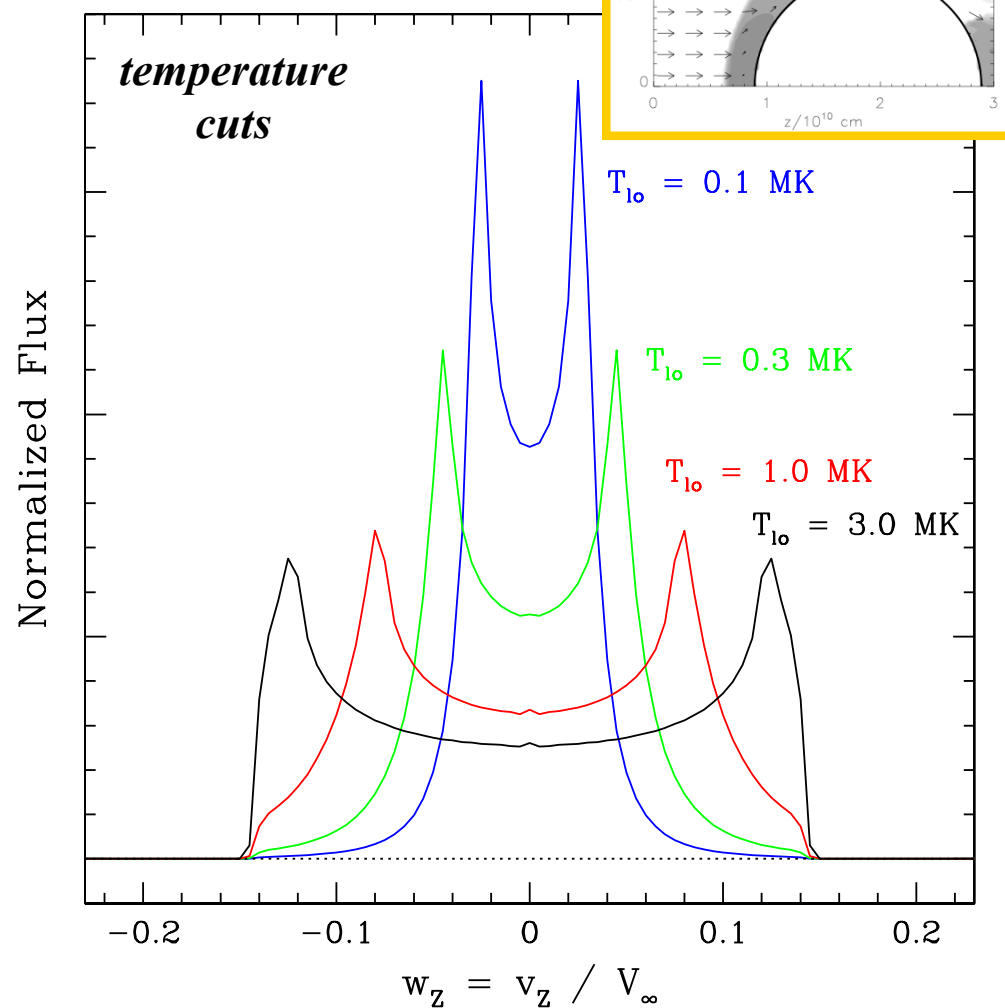


Figure 3. Similar to Figure 2 but now profiles are for clumps only at $\vartheta = 90^\circ$ and with different temperature intervals. The emissivity is taken to be constant within the temperature range of T_{lo} up to T_A , with $T_{lo} = 0.1, 0.3, 1.0,$ and 3.0 MK from the most narrow line (blue) to the broadest one (black), respectively.

increasing number
of clump bowshocks
randomly distributed
throughout the wind
as 2^n

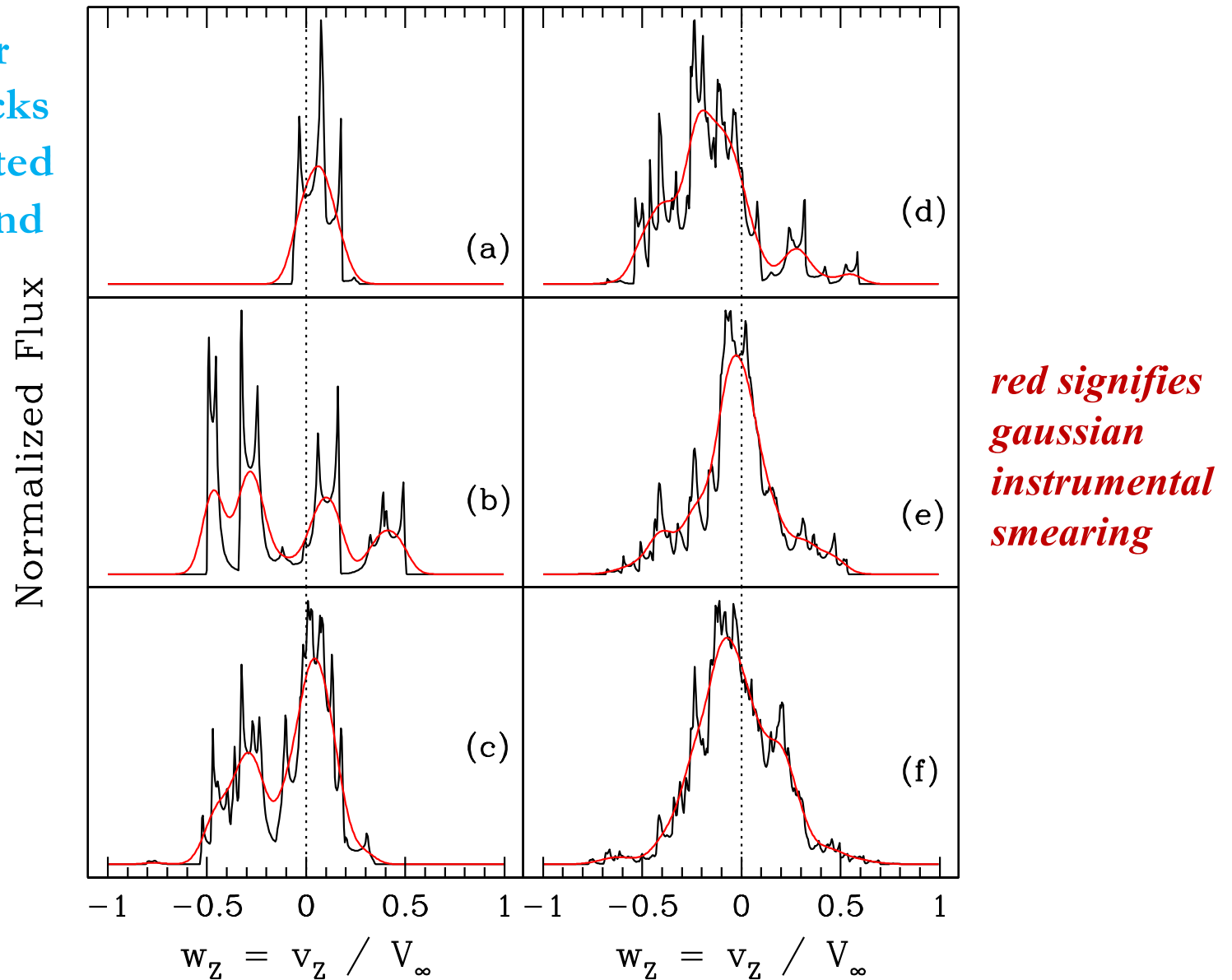


Figure 7. Line profile shapes for an ensemble of clumps with $\tau_* = 0.1$. Panels are distinguished by the number of clumps \mathcal{N}_{cl} used in the model, with (a) 4, (b) 8, (c) 16, (d) 32, (e) 64, and (f) 128 clumps. Model line profiles are shown in black; overplotted are red curves that include the effects of instrumental smearing are included. Finite spectral resolution is approximated by convolving model lines with a Gaussian that has $\sigma = 0.05V_\infty$.

Testing the reliability of X-rays as a tool for constraining mass-loss rates of hot stars

Sean J. Gunderson ¹*, Kenneth G. Gayley ¹, Pragati Pradhan ², David P. Huenemoerder ²
and Nathan A. Miller ³

Source Effects

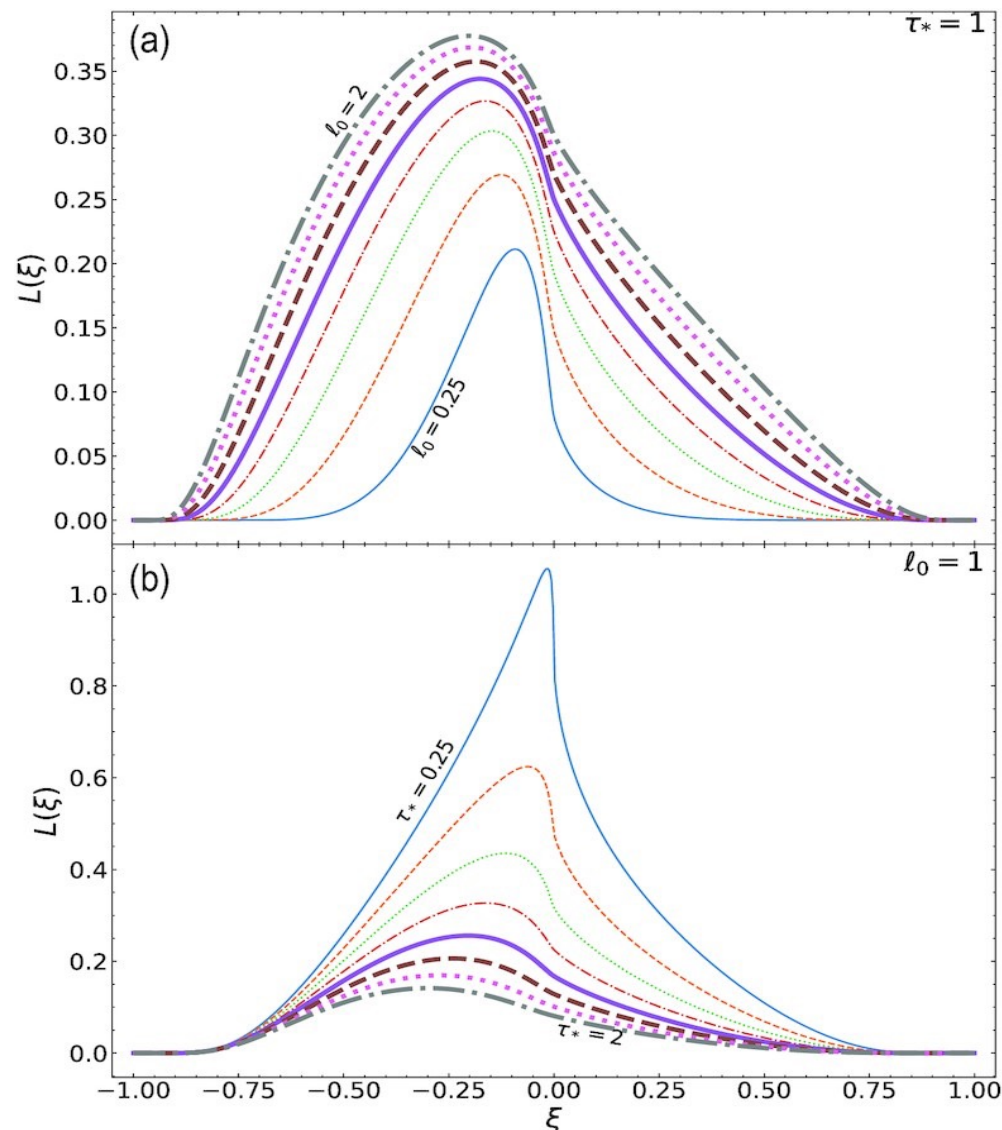
Line profile calculation depends on **TWO** main ingredients:

- source distribution (choices)
- escape distribution (choices)

Most line modeling proceeds on assumption of ρ^2 emissivity; Gunderson+ have proposed prompt energy dump by wind shocks.

Gunderson+ 2023:

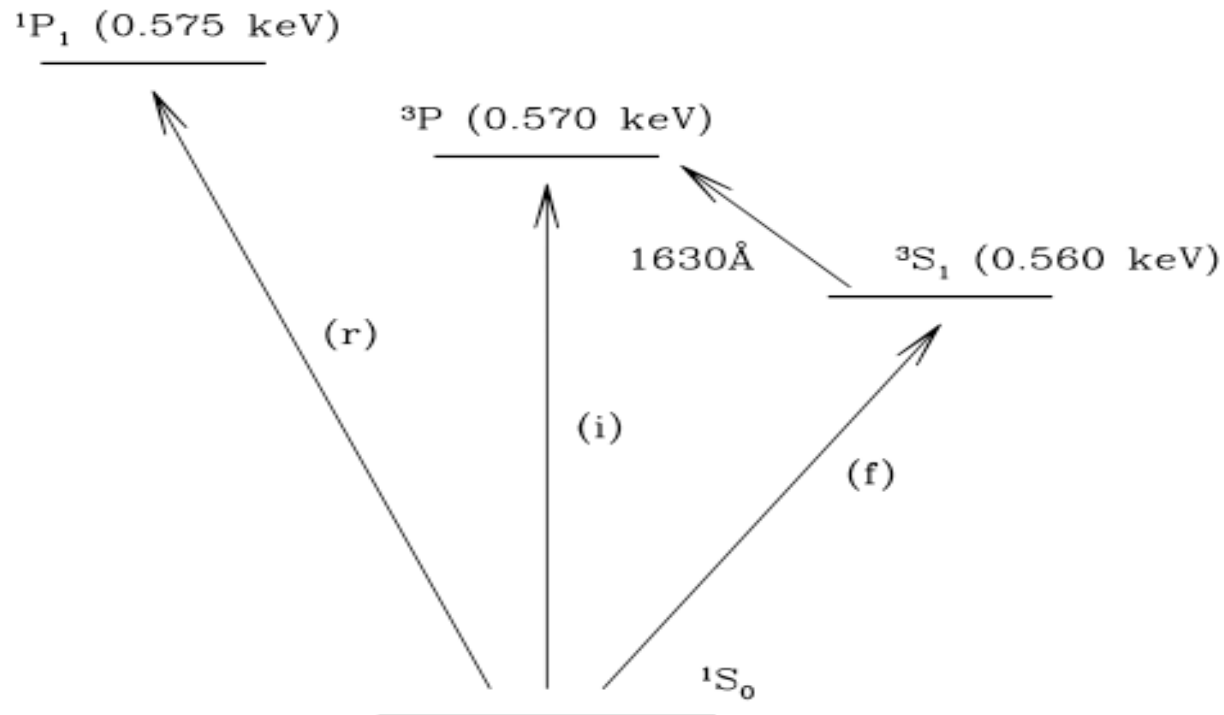
$$\frac{dL}{d\xi} = 4\pi \int j_\nu e^{-\tau} dV$$
$$\sim \int \frac{1}{v(r)} \frac{e^{-(r-R)/l_0}}{l_0} e^{-\tau} dr$$



Multiplet Effects: *Proximity Diagnostic from f/i ratios*

He-like triplets normally yield density and temperature diagnostics; however, UV pumping from hot stars ends up yielding a *location* diagnostic (via the dilution factor).

He-like Triplet of OVII

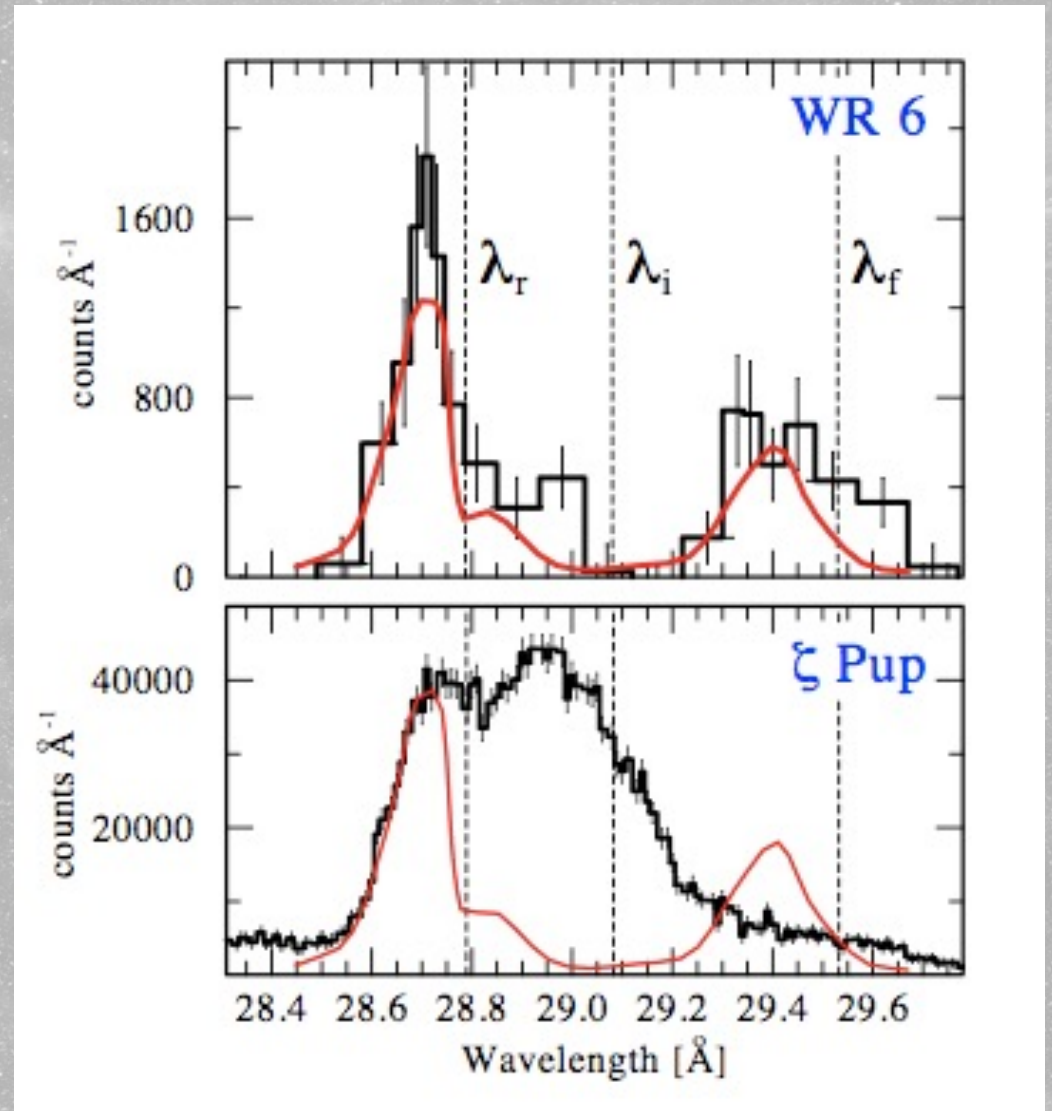


r=resonance, i=intercombination, f=forbidden

Example Application of He-like Triplets

OB stars like zeta Pup typically show a suppressed forbidden component owing to UV pumping effects

XMM/RGS data of WR6 shows normal ratios, indicating an absence of UV pumping and supporting line formation at (somewhat) large radii



Modeling f-i-r Lines

Chandra has not been able to resolve the separate triplets for winds

$$\tilde{R} = R_0 \frac{1}{1 + 2k_* W(r)}$$

R_0 is without UV pumping

$$\frac{dL}{dv_{obs}} = 4\pi \int j_\nu w_x e^{-\tau} \frac{dV}{v}$$

emission line calculation

$$w_{fir} = \begin{cases} \frac{\tilde{R}(r)}{1 + \tilde{R}(r)} \\ 1 \\ \frac{1}{1 + \tilde{R}(r)} \\ 1 \end{cases}$$

f-i-r weighting factors

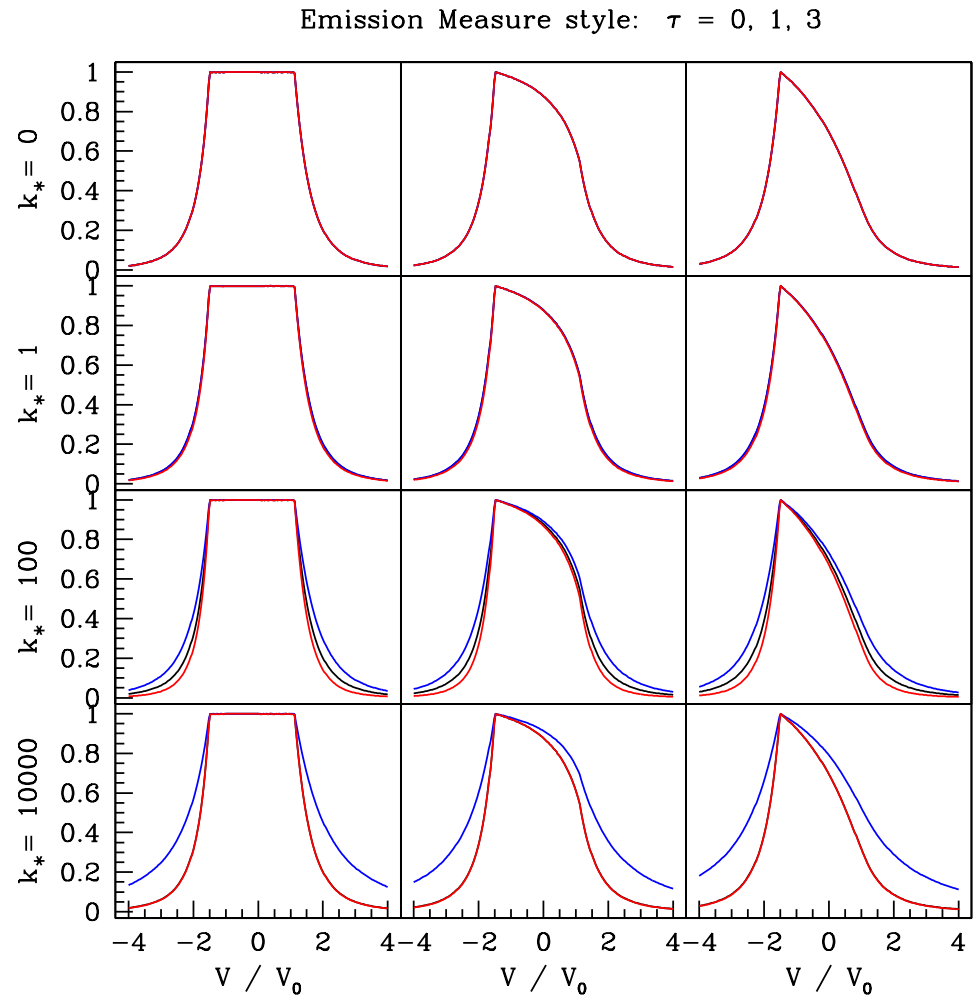
f-i-r Profile Shapes for hi-res

Level of pumping is distance dependent and imposes differential imprints on the 3 line component profiles

Hi-resolution could provide new ways of probing the velocity field of the hot plasma (here $v \sim r$ assumed)

General rule for broadening of peak normalized profiles:
i-line narrowest and
f-line broadest

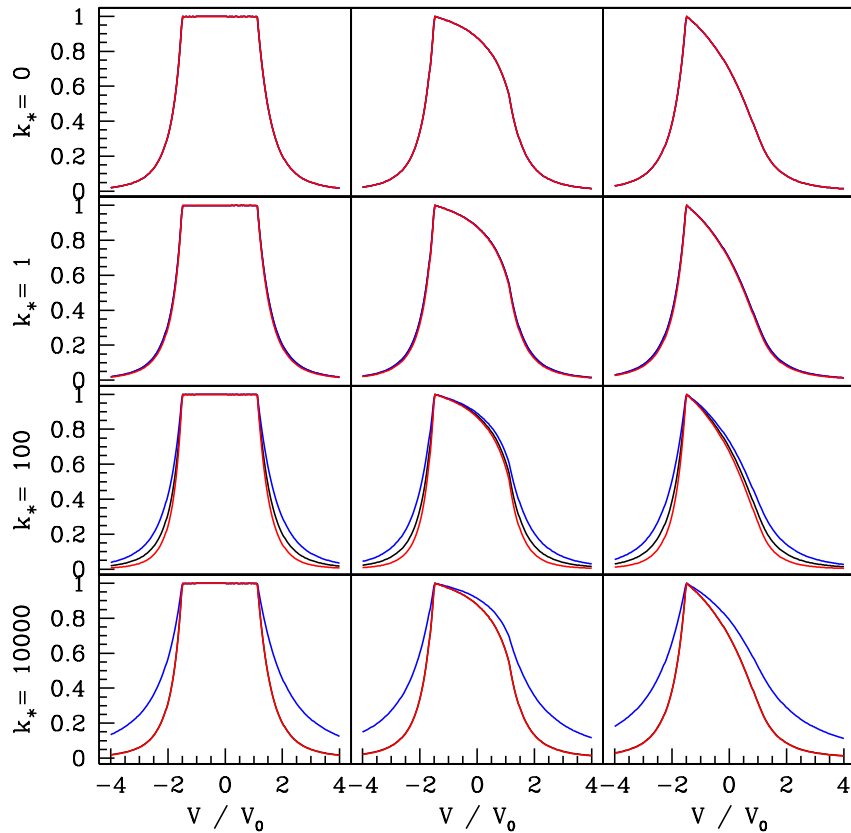
Note: peak normalized for comparison of shapes



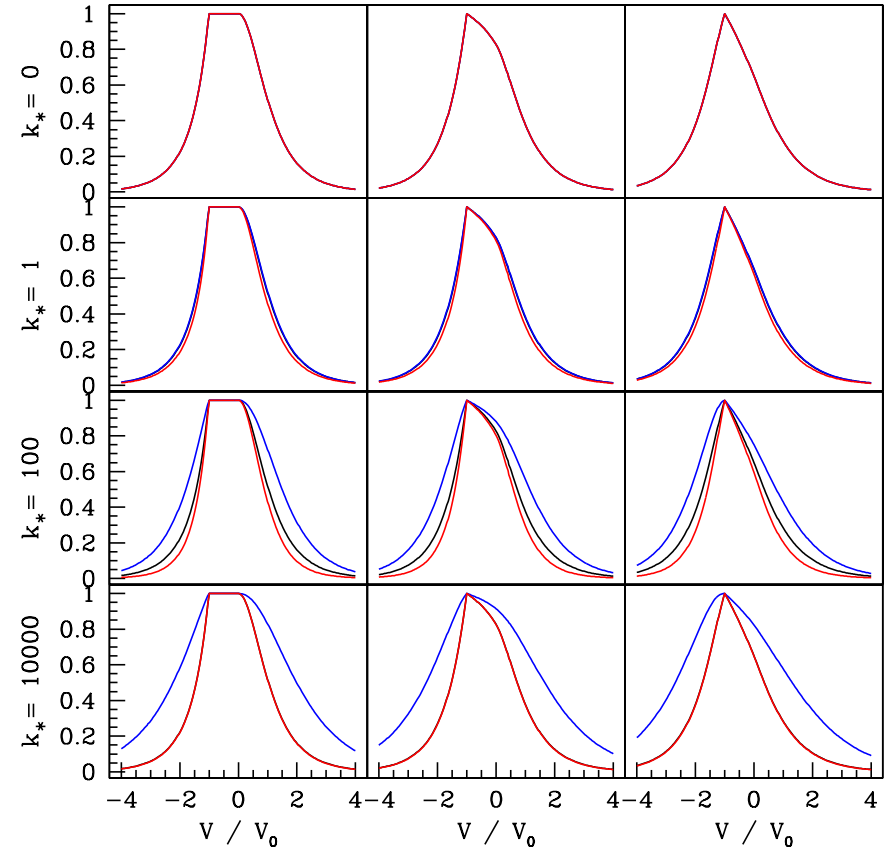
red is i-line; black is r-line; blue is f-line

Some f-i-r Profile Possibilities

Emission Measure style: $\tau = 0, 1, 3$



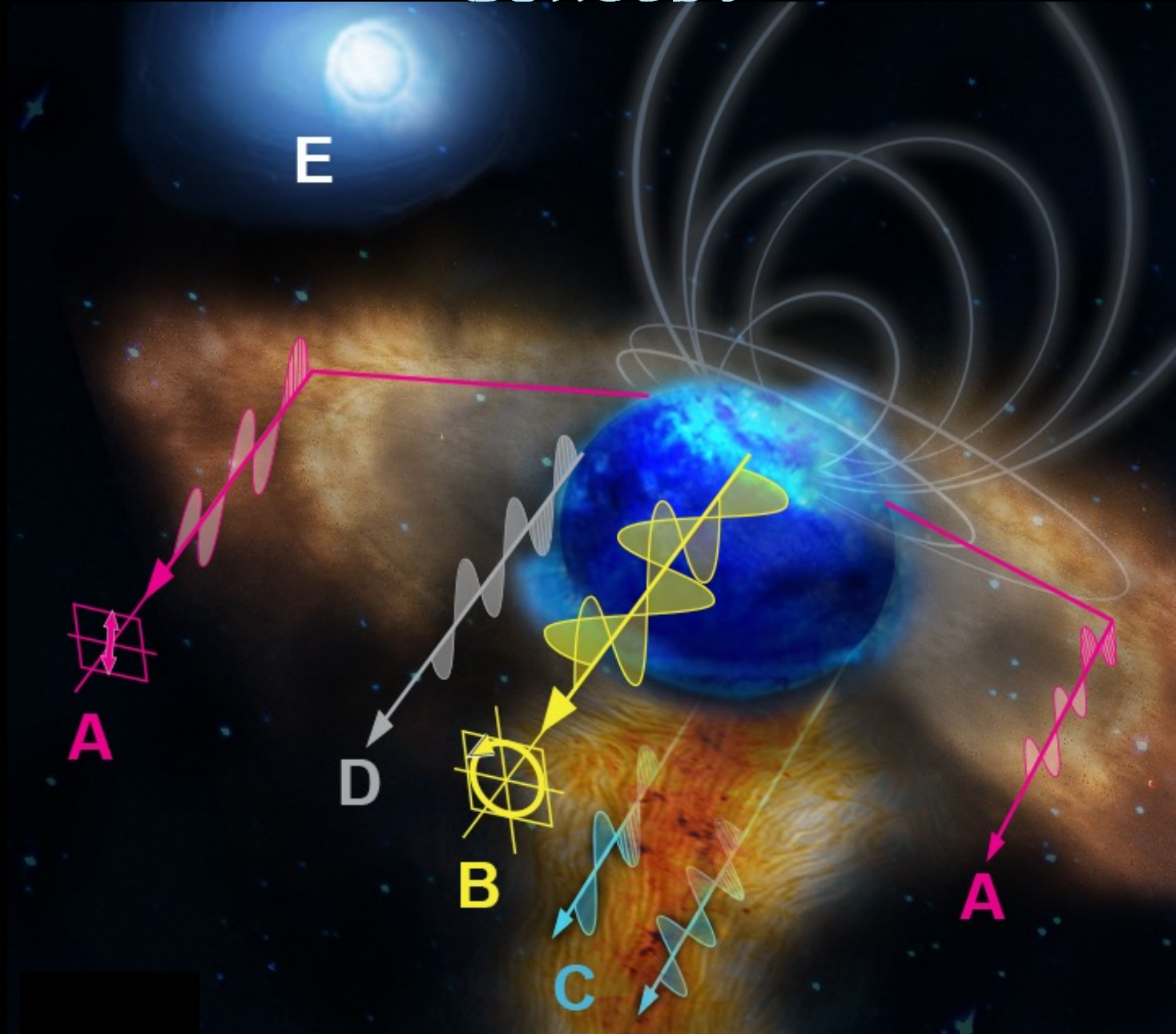
Gunderson+ style: $\tau = 0, 1, 3$



f-line is broad because emission is weak!!!

➡ **photon-starved diagnostic**

Polstar UV Spectropolarimetry Mission Concept



Thank you!

QUESTIONS?

SUMMING UP

Large X-ray telescopes and their unprecedented spectral capability continue to make this an exciting time for the study of the driving and structure of massive star winds. Yet more can be achieved with future missions.

- **X-rays probe shocks in massive star circumstellar environs**
- **Wind-shock paradigm for OB stars seems in decent shape (zeta Pup continuum and line shape modeling)**
- **X-rays from WR stars emerge from large radius (WR6 line shapes)**
- **Clumping continues to be of interest on many levels, from potential porosity effects for escape of X-rays, to clump bowshocks for detailed wind structure**
- **Some of the best-quality O star X-ray data come from reasonably fast rotators – time for new considerations of rotational effects?**
- **Source model approaches for shock X-rays appears ongoing**
- **f-i-r lines offer a variety of diagnostic potential (some not covered)**
- **Not covered:** Line profiles probe bowshocks of colliding winds with orbital phase; connects observations to hydro simulations